Aη-α and Aη-β peptides impair LTP ex vivo within the low nanomolar range and impact neuronal activity *in vivo*.

Maria Mensch
CNRS UMR7275
Jade Dunot
CNRS UMR7275
Sandy Yishan
CNRS UMR7275
Samuel Harris
UK dementia Institute at UCL
Aline Blistein
Goethe-Universitat Frankfurt am Main
Alban Avdiu
Goethe-Universitat Frankfurt am Main
Paula A Pousinha
CNRS UMR7275
Camilla Giudici
German Centre for Neurodegenerative Diseases Munich: Deutsches Zentrum fur Neurodegenerative Erkrankungen Standort Munchen
Marc Aurel Busche
UK demential Research Institute at UCL
Peter Jedlicka
Goethe-Universitat Frankfurt am Main
Michael Willem
LMU München: Ludwig-Maximilians-Universitat Munchen
Helene Marie (marie@ipmc.cnrs.fr)
CNRS UMR7275 https://orcid.org/0000-0003-2310-6097

Research Article

Keywords: APP processing, synaptic plasticity, electrophysiology, hippocampus, Alzheimer

Posted Date: March 10th, 2021

DOI: https://doi.org/10.21203/rs.3.rs-259533/v1

Version of Record: A version of this preprint was published at Alzheimer's Research and Therapy on July 8th, 2021. See the published version at https://doi.org/10.1186/s13195-021-00860-1.

Abstract

Background

Amyloid precursor protein (APP) processing is central to Alzheimer's disease (AD) etiology. As early cognitive alterations in AD are strongly correlated to abnormal information processing due to increasing synaptic impairment, it is crucial to characterize how peptides generated through APP cleavage modulate synapse function. We previously described a novel APP processing pathway producing η-secretase-derived peptides (Aη) and revealed that Aη−α, the longest form of Aη produced by η-secretase and α-secretase cleavage, impaired hippocampal long-term potentiation (LTP) *ex vivo* and neuronal activity *in vivo*.

Methods

With the intention of going beyond this initial observation, we performed a comprehensive analysis to further characterize the effects of both Aη-α and the shorter Aη-β peptide on hippocampus function using *ex vivo* field electrophysiology, *in vivo* multiphoton calcium imaging and *in vivo* electrophysiology.

Results

We demonstrate that both synthetic peptides acutely impair LTP at low nanomolar concentrations *ex vivo* and reveal the N-terminus to be a primary site of activity. We further show that Aη-β, like Aη−α, inhibits neuronal activity *in vivo* and provide confirmation of LTP impairment by Aη−α *in vivo*.

Conclusions

These results give novel insights into the functional role of the recently discovered η-secretase-derived products, and suggest that Aη peptides represent important, pathophysiologically relevant, modulators of hippocampal network activity, with profound implications for APP-targeting therapeutic strategies in AD.

Background

The amyloid precursor protein (APP) is a transmembrane protein that is highly expressed in neurons of the developing and adult brain. Due to its location at synaptic and perisynaptic sites[1] it is ideally positioned to regulate synaptic signaling. At these sites, APP is cleaved into a variety of secreted and intracellular peptides through the action of different proteases[2]. We previously reported the discovery of an additional APP processing pathway involving a novel cleavage site, N-terminal to the β-secretase-1 (BACE1) cleavage site. This site is targeted by an enzymatic process that we named η-secretase and potentially mediated by membrane types 1 and 5 matrix metalloproteinases (MT1-MMP and MT5-MMP)[3]. APP processing via this pathway leads to the generation of two secreted Aη peptides: a longer form Aη−α and a comparatively shorter form Aη−β that are generated by η-secretase cleavage and subsequent α-secretase or β-secretase cleavage, respectively[3]. APP cleavage is a physiological process which occurs throughout life, with Aη peptides being detected both in adult healthy human and rodent brain tissue[3]. Aη peptides are present in the cerebrospinal fluid (CSF) of healthy humans and, notably, exceed Aβ levels five-fold. Their preponderance suggests that Aη peptides might act as endogenous modulators of neuronal network activity, although this hypothesis remains to be proven. Furthermore, since pathological alterations in APP processing are crucially involved in the etiology of AD[2], unravelling the function of Aη peptides might help to elucidate the pathophysiological mechanisms of homeostatic failure, including defective synapse communication, underlying cognitive decline typical of AD[4–6]. Finally, BACE1 inhibition is currently evaluated as a potential therapeutic strategy to lower Aβ load in AD patients and prevent cognitive decline. However, we previously demonstrated that BACE-1 inhibition increases levels of Aη peptides[3]. It will thus be important to thoroughly identify their neuromodulatory potential in order to avoid adverse side effects due to this type of treatment.

Beyond reporting the discovery of these Aη peptides, our initial work provided the first insights on their impact on neuron function. Then, we observed that both cell-produced recombinant Aη−α (recAη−α) and synthetic Aη−α (sAη−α) lowered hippocampal long-term potentiation (LTP) *ex vivo* and reduced spontaneous somatic calcium transients of hippocampal neurons *in vivo*[3], while recombinant cell-produced Aη−β (recAη−β) did not have any impact on these parameters. Here, we combined *ex vivo* field electrophysiology, *in vivo* multiphoton calcium imaging, and *in vivo* electrophysiology to further characterize the impact of both Aη−α and Aη−β on hippocampal function.

Methods

Animals

For *ex vivo* electrophysiology recordings, 4–8 weeks old male RjOrl:SWISS mice were used. Experiments were conducted according to the policies on the care and use of laboratory animals stipulated by French ministry of research according to the European Communities Council Directive (2010/63).

For *in vivo* LTP experiments, all injections and recordings were performed on adult male Sprague-Dawley rats (450–650 g). The experiments were performed in accordance with local institutional and governmental regulations regarding the use of laboratory animals at the University of Frankfurt as approved by the Regierungspräsidium Darmstadt and the animal welfare officer responsible for the institution.

For *in vivo* calcium imaging experiments, male and female C57Bl/6 mice (~ 40) were used. Experiments were conducted in compliance with institutional (Technische Universität München) animal welfare guidelines and approved by the state government of Bavaria, Germany.

Peptides

Synthetic Aη peptides were obtained from Peptide Specialty Laboratories (PSL GmbH; Heidelberg, Germany) and consisted of the following sequences:

Synthetic Aη−α (sAη−α, 108 amino acids) sequence:

MISEPRISYGNDALMPSLTETKTTVELLPVNGEFSLDDLQPWHSFGADSVPANTENEVEPVDARPAADRGLTTRPGSGLTNIKTEEISEVKMDAEFRHDSGYEVHHQK

Synthetic A□−β (sAη−β, 92 amino acids) sequence:

MISEPRISYGNDALMPSLTETKTTVELLPVNGEFSLDDLQPWHSFGADSVPANTENEVEPVDARPAADRGLTTRPGSGLTNIKTEEISEVKM
Synthetic N-term sAη (sAη−NT, 46 amino acids) sequence:

MISEPRISYGNDALMPSLTETKTTVELLPVNGEFSLDDLQPWHSFG
Synthetic C-term sAη−β (sAη−β−CT; 46 amino acids) sequence:

ADSVPANTENEVEPVDARPAADRGLTTRPGSGLTNIKTEEISEVKM
The peptides were dissolved in dimethyl sulfoxide (DMSO) at 100 µM and placed at − 80°C for long term storage. For *ex vivo* electrophysiology, on day of experiment, aliquots were further diluted in artificial cerebrospinal fluid (aCSF) (see below) to the required concentration (1–10 nM).

For *in vivo* electrophysiology, aliquots were further diluted on day of experiment in phosphate buffered saline (PBS) to the required concentration (1 µM).

For *in vivo* calcium imaging, the peptides were combined with Ringer's solution (see below) on day of experiment to 100 nM.

Recombinant Aη peptides were generated and purified as described previously[3]. Briefly, for the expression of Aη−α and Aη−β in CHO cells, the complementary cDNAs of the respective fragments were amplified by PCR and subcloned into the pSecTag2A (Invitrogen) vector that features an N-terminal secretion signal. CHO cells were cultured in DMEM with 10% FCS and non-essential amino acids. Transfections were carried out using Lipofectamine2000 (Invitrogen) according to the manufacturer's instructions. The next day media was changed to OPTIMEM (Invitrogen) and the serum free conditioned media of the transfected cells, expressing the recombinant Aη peptides, were collected after 20 hours. Up to 1 liter of C-terminally HIS-tagged peptides were purified by anion exchange chromatography using *HiTrap* columns for small-scale protein purification (Cytiva) (Ni-NTA purification)[3]. Positive fractions were pooled and the elution buffer was exchanged using Vivaspin 20 MWCO3centrifugation tubes (Sartorius) with 3 volumes of aCSF. The protein concentration was measured based on the OD280 with a Nanodrop device (Thermo Fisher) and calculated for each protein based on the molecular weight of the nonglycosylated peptide including the myc-HIS tag. The preparation was diluted to a final concentration of 10nM in ACSF on day of experiment.

Protein analysis

10ng of recombinant Aη−α and Aη−β were loaded onto a precast gradient Tricine Protein Gel (10–20%, 1 mm, Novex) in Tris-tricine buffer using the mini gel tank system (Invitrogen). After separation by SDS−PAGE, proteins were transferred onto a nitrocellulose membrane (Protran BA85; GE Healthcare) using the tank/wet Mini Trans-Blot cell system (BIORAD). After completion of the transfer, membranes were boiled in PBS (140mM NaCl, 10mM Na_2HPO_4, 1.75mM KH_2PO_4, 2.7mM KCl in ddH_2O, pH 7.4) for 5 min. Then, membranes were blocked in I-Block solution (0.2% Tropix I-Block (Applied Biosystems), 0.1% Tween20 in PBS) for 1 h at room temperature. Membranes were incubated with 2E9 primary antibody[1] (1/1000) in I-block solution overnight. Membranes were washed three times in PBS/0.1% Tween20 (PBS-T) buffer (10 min each, at room temperature, with agitation; 0.2% Tween20 in PBS). Membranes were incubated with a horseradish peroxidase-coupled secondary antibody (rat,1/5000, Sigma A5795) in I-Block solution for 1h at room temperature (with agitation) followed by three washes in PBS-T. Transferred proteins were detected using immunodetection and enhanced chemiluminescence (ECL ultra, Perkin Elmer) with incubation of membrane for 1 min at room temperature and signals were captured for 2s.

Ex vivo electrophysiology

Mice were culled by cervical dislocation and hippocampi were dissected and incubated for 5 min in ice-cold oxygenated (95 % O_2/ 5 % CO_2) cutting solution (in mM): 206 sucrose, 2.8 KCl, 1.25 NaH_2PO_4, 2 $MgSO_4$, 1 $MgCl_2$, 1 $CaCl_2$, 26 $NaHCO_3$, 10 glucose, 0.4 sodium ascorbate, oxygenated with 95 % O_2 and 5 % CO_2, (pH 7.4). Hippocampal slices (350 µm) were cut on a vibratome (Microm HM600V, Thermo Scientific, France). For recovery, slices were then incubated in oxygenated aCSF for 1 h at 37 ± 1°C and then stored at room temperature until used for recordings. aCSF composition was (in mM): 124 NaCl, 2.8 KCl, 1.25 NaH_2PO_4, 2 $MgSO_4$, 3.6 $CaCl_2$, 26 $NaHCO_3$, 0.4 sodium ascorbate, 10 glucose, oxygenated with 95 % O_2 and 5 % CO_2, pH 7.4. All

chemicals were from Sigma-Aldrich (Saint-Quentin Fallavier, France). Recordings for all experiments were done at 27 ± 1°C in a recording chamber on an upright microscope with IR-DIC illumination (SliceScope, Scientifica Ltd, UK). Field recordings were performed using a Multiclamp 700B amplifier (Molecular Devices, San Jose, CA, USA), under the control of pClamp10 software (Molecular Devices, San Jose, CA, USA). Data analysis was executed using Clampfit 10 software (Molecular Devices, San Jose, CA, USA). Field excitatory post-synaptic potentials (fEPSPs) were recorded in the stratum radiatum of the CA1 region (using a glass electrode filled with 1 M NaCl and 10 mM 4-(2-hydroxyethyl)-1-piperazineethanesulfonic acid (HEPES), pH 7.4) and the stimuli were delivered to the Schaffer collateral pathway by a monopolar glass electrode filled with aCSF. fEPSP response was set to approximately 30 % of the maximal fEPSP response i.e. approx. 0.2–0.3 mV, with stimulation intensity 10 µA ± 5 µA delivered via stimulation box (ISO-Flex, A.M.P.I. Inc., Israel). Electrodes were placed superficially to maximize exposure to peptides. Slices were perfused with oxygenated aCSF. A stable baseline of 15–20 min bath application of aCSF under control conditions or with synthetic or recombinant peptide was first obtained before induction for LTP. The peptide was then also recirculated throughout the one-hour recording after induction. LTP was induced by a high frequency stimulation (HFS) protocol: 2 pulses at 100 Hz for 1 s with a 20 s inter stimulus interval (ISI).

For all LTP recordings, only the first third of the fEPSP slope was analyzed to avoid population spike contamination. The time courses of LTP were obtained by normalizing each experiment to the average value of all points constituting a 15–20 min stable baseline before induction. LTP magnitude was measured during the last 15 min of recording (45–60 min after induction) and calculated as % change fEPSP slope from baseline average. Recordings of control and peptide conditions were interleaved within the same day.

In vivo electrophysiology

Urethane (Sigma-Aldrich GmbH, Munich, Germany) solution was used to anaesthetize the animals with an initial injection (2 g/kg body weight) applied intraperitoneally. Supplemental doses (0.2–0.5 g/kg) were injected subcutaneously until the interdigital reflex could no longer be triggered. The body temperature of the animal was constantly controlled through a rectal probe and maintained at 36.5–37.5°C using a heating pad. For local anaesthesia of the scalp prilocaine hydrochloride with adrenalin 1:200,000 (Xylonest 1 %, AstraZeneca GmbH, Wedel, Germany) was injected subcutaneously at the site of incision. The head of the anesthetized rat was placed into a stereotaxic frame for accurate insertion of electrodes and injection cannula. Using standard surgical procedures, we drilled the stimulation and recording holes and removed the dura mater. A tungsten recording micro-electrode glued to a 10 µl Hamilton series syringe was lowered unilaterally into the dentate gyrus hilus (2.5 mm lateral and 3.8 mm posterior to bregma), and a bipolar concentric stimulating electrode was lowered unilaterally into the perforant path (4.5 mm lateral to lambda), while monitoring the laminar profile of the response. Current pulses (30–800 µA, 0.1–0.2 ms duration) were generated by a stimulus generator (STG1004, Multichannel Systems, Reutlingen, Germany). The recorded fEPSPs were first amplified (P55 preamplifier, Grass Technologies, West Warwick, RI, USA) and then digitized at 10 kHz for visualisation and offline analysis (Digidata 1440A, Molecular Devices, San Jose, CA, USA). The analysis of electrophysiological data was executed using Clampfit 10.2 software (Molecular Devices, San Jose, CA, USA) as well as custom MATLAB scripts (The MathWorks, Natick, MA, USA). As a measure of synaptic LTP, we compared responses with baseline stimulation prior to theta-burst stimulation (TBS) with responses subsequent to TBS. At the start of each experiment, stable baselines were recorded. Then, the experimental solution was injected into the hippocampus. In each experiment, injections of 1 µl of sAη–α or sAη–β–CT (1 µM) were delivered from the Hamilton syringe attached to a microinjection unit (Model 5000, Kopf Instruments, Tujunga, CA, USA). Intradentate injections of fluid led to a typical temporary reduction in the fEPSP slope and amplitude, probably caused by changes in extracellular resistivity[7]. The degree of response suppression and recovery can be seen in LTP graphs. After a baseline period of 20 min, LTP was induced using a standard TBS protocol: six series of six trains of six pulses at 400 Hz, with 0.2 s between trains and 20 s between series. Both the pulse width and the stimulus intensity during TBS were doubled in comparison to baseline recordings. The LTP was followed for 60 min using the baseline stimulation protocol. For the analysis of the slope of the fEPSP, only the early component of the waveform, which is not affected by the population spike, was used. LTP was calculated as an average of the 60 min post TBS. The potentiation of the fEPSP slope was expressed as a percentage change relative to the pre-TBS baseline.

In vivo multiphoton calcium imaging

The procedure for animal preparation followed the same protocol as described previously[3,8]. Briefly, C57Bl/6 mice were placed in an induction box and anesthetized using isoflurane (~ 3–4 %). Following induction, animals were transferred to a stereotaxic frame and heating plate (37–38°C) and maintained using 1–1.5 % isoflurane during surgical procedures, with respiration and pulse rate continuously monitored. The skin was first carefully excised and retracted, and a custom-made recording chamber/well affixed to the exposed skull. Subsequently, a small craniotomy (1 mm^2, 2.5 mm posterior to bregma, 2.2 mm lateral to the midline) was performed and the exposed cortical tissue carefully aspirated to reveal the underlying hippocampus (CA1). The recording chamber was perfused with warmed Ringer's solution (in nM): 125 NaCl, 4.5 KCl, 26 $NaHCO_3$, 1.25 NaH_2PO_4, 2 $CaCl_2$, 1 $MgCl_2$ and 20 glucose, pH 7.4, 95 % O_2 and 5 % CO_2, and the hippocampus stained using Fluo-8®, AM (0.6 mM) (AAT Bioquest, Inc., Sunnyvale, CA, USA) via the multi-cell bolus loading injection technique[9]. Peptides (100 nM) were perfused into the recording chamber for bath application to the exposed CA1 region of the hippocampus (45–60 min wash in). *In vivo* imaging was conducted as described previously using a custom-built two-photon microscope consisting of a titanium:sapphire laser (Coherent; λ = 925 nm), resonant scanner, a Pockels cell laser modulator, and a water-immersion objective (Nikon; 40× 0.8 numerical aperture)[1]. Images were acquired at a sampling rate of 30 Hz using custom-written LabVIEW routines and analyzed off-line in LabVIEW (National Instruments, Austin, Texas, USA), Igor Pro (WaveMetrics, Inc., Lake Oswego, OR, USA) and MATLAB (The MathWorks, Natick, MA, USA). Regions of interest (ROIs) were manually defined around individual cell-bodies, and time-series of relative calcium fluorescence

changes (ΔF/F) were extracted for each ROI. Significant changes in fluorescence were defined as ΔF/F calcium transients which exceeded background noise levels by > 3 standard deviations (SD). Animals were maintained at low levels of isoflurane anesthesia (~ 0.8 %) throughout imaging procedures.

Statistical analysis

Results are shown as mean ± S.E.M. For *ex vivo* and *in vivo* electrophysiology, statistical analyses were performed with Prism GraphPad 6.0 Software (GraphPad Software, La Jolla, CA, USA) and are presented in detail in supplementary Tables S1–S5. The normality of the data distribution was verified with the Shapiro-Wilk's test. Unpaired Student's two-tailed t-test was used for comparison of two independent samples and two-way RM ANOVA followed by Sidak's post-hoc test were used for multiple comparisons of more than two conditions for *ex vivo* electrophysiology. 'N' refers to number of animals and 'n' to the number of slices examined.

For *in vivo* electrophysiology, unpaired Student's two-tailed t-test was used for comparison of two independent samples. 'N' refers to number of animals.

Statistical analyses of *in vivo* calcium imaging data were performed using MATLAB (The MathWorks, Natick, MA, USA). Following testing for normality using a one-sample Kolmogorov-Smirnov, the non-parametric Mann-Whitney U-test was used to test for equality of population medians. For statistical testing of more than two groups, the nonparametric Kruskal-Wallis test was used with Tukey-Kramer correction for multiple comparisons. The experimenter was blinded to the synthetic peptide being administered and corresponding data only decoded at the end of experimentation. Significant effects were inferred at $p < 0.05$.

Results

sAη−α and sAη−β impair LTPex vivo**within low nanomolar range**

Previously, we reported an impairment of LTP at the CA3−CA1 synapse upon acute exposure of adult mouse hippocampal slices to synthetic Aη−α (sAη−α) at 100 nM[3]. We now report that synthetic Aη−β (sAη− β) also lowers LTP at 100nM (Fig. 1a-b). To exclude putative high-dose concentration-related toxicity, we now aimed to identify the minimal dose at which both sAη-α and sAη−β can affect LTP. Application of both 10 nM and 5 nM was sufficient to significantly reduce LTP response compared to control conditions (Fig. 1c-f), an effect which did not persist at 1 nM (Fig. 1g-h). We conclude that these peptides are active within the low nanomolar range.

10nM of recombinant Aη−β impairs LTPex vivo

We previously reported that recombinant forms of these peptides, produced from CHO cell (Fig. 2a-b), differently impacted LTP *ex vivo* with recAη−α but not rec Aη−β lowering LTP[3]. Of note, at the time, we had not carefully assessed the concentration of the recombinant peptides that were applied during LTP analysis. As we now report that the synthetic form of the Aη−β peptide lowers LTP (Fig. 1), a result in direct contradiction with this previous finding, we repeated the previously published experiment by exposing hippocampal slices to 10nM of recAη−α or recAη−β, after careful evaluation of the final concentration of the purified proteins with equal amounts detected by Western blot analysis as shown in Fig. 2b. Here, we report that, at this dose, like their synthetic counterparts, both recombinant peptides significantly lower LTP (Fig. 2c-d).

N-terminus sequence of Aη is necessary and sufficient for LTP impairment

Next, we aimed at identifying the region in Aη that mediates the effect on LTP. We synthesized two other peptides (46 amino acids each) representing the N-terminal and C-terminal portions of sAη−β, that we termed sAη−NT and sAη−β−CT, respectively (Fig. 3a). Whereas sAη−NT (100 nM), comprising the N-terminal stretch of amino acids present in both sAη−α and sAη−β, lowered LTP, sAη−β−CT (100 nM) failed to recapitulate this effect (Fig. 3b-c). Taken together, these findings indicate that the N-terminal part of Aη is necessary and sufficient for LTP impairment.

sAη peptides induce hippocampal neuronal hypoexcitabilityin vivo

We previously reported that sAη−α (100 nM) suppressed neuronal activity *in vivo* by using multiphoton calcium imaging at single cell resolution[3]. Here we performed the same experiment using sAη−β, with sAη−β−CT as the control peptide, and reanalyzed our previously published data[1] in order to compare the effects of sAη−α and sAη−β versus sAη−β−CT (all 100 nM). We found that sAη−α and sAη−β superfusion ('wash-in') resulted in a significant reduction in neuronal activity, as measured by the spontaneous frequency of calcium transients in CA1 from baseline, with no significant effects induced by the N-terminally truncated control peptide sAη−β−CT (Fig. 4a−d). In contrast to sAη−β−CT, both sAη−α and sAη−β were associated with an increase in the number of silent neurons (Fig. 4e), indicating that both synthetic Aη peptides induce profound neuronal hypoexcitability *in vivo*.

sAη−α also lowers LTPin vivo

Finally, to assess whether sAη−α also impairs long-term synaptic plasticity in the intact circuitry of live animals, we tested its impact on LTP in the hippocampus *in vivo*. For this purpose, 1 μM sAη−α was acutely applied into the hippocampal dentate gyrus of urethane-anaesthetized rats. As a control peptide, we used sAη−β−CT (1 μM) that did not impact LTP *ex vivo* (Fig. 3) nor neuronal activity i*n vivo* (Fig. 4). LTP was induced by TBS of perforant path synaptic inputs in the dentate gyrus[10,11]. TBS was applied after a typical transient decline and recovery of baseline fEPSP responses upon the brief injection of 1 μl fluid containing sAη−α or control peptide (see Fig. 5a and Methods). Following TBS, significant LTP of the fEPSPs was

observed in both groups of rats. However, sAη−α efficiently lowered LTP when compared its control peptide during both the induction (Fig. 5b) and maintenance (Fig. 5c) of LTP. These data demonstrate that sAη−α is also able to reduce LTP in the living brain.

Discussion

In this report, we provide important novel insights into the activity of Aη peptides at excitatory hippocampal synapses. Notably, we demonstrate that both the long and short forms of Aη are active within the low nanomolar range that is strongly indicative of physiological relevance. Specifically, we report that the recombinant form of the Aη−β lowers LTP, provide confirmation of the impact of sAη−α on LTP in the intact brain, and show that, like sAη−α, sAη−β also induces neuron hypoexcitability *in vivo*, suggesting that both peptides share a similar bioactive profile. Finally, we provide novel evidence that the active region of Aη is located within its N-terminus sequence.

The Aη-dependent impairment of LTP is reminiscent of the activity of Aβ, in its dimer or oligomeric forms, at these same synapses [12–14]. Aη−α overlaps with the N-terminus of Aβ by 16 amino acids and it thus may be tempting to speculate that Aη−α−mediated effects on synaptic plasticity reflect a common active site. Yet, our data do not support this interpretation for several reasons. First, we found a similar LTP impairment with sAη−β, which does not harbor these overlapping 16 amino acids. Second, the likelihood of the active site lying in N-terminal portion of the Aη sequence was supported by our observation that, while both sAη−NT and sAη−β−CT are present in Aη peptides but not in Aβ, only sAη−NT lowered LTP *ex vivo*. Finally, the effects of Aβ on LTP are only observed with aggregated Aβ[14,15], in contrast to the monomeric activity of Aη peptides, which mediate these effects since these peptides does not oligomerize[3].

Our finding that Aη peptides impact LTP and neuronal excitability within the low nanomolar range emphasize that care should be taken when designing therapeutic strategies for AD, such as when increasing Aη−α brain levels through BACE-1 inhibition[3]. Furthermore, since BACE-1 inhibition would also be expected to increase the generation of soluble APP species (sAPPα), recently reported to reduce neuronal activity *in vivo*[16], the resulting suppressive effect of both peptide species on neuronal activity might well be pronounced, and may partly explain observations of acute adverse cognitive outcomes in recent BACE-1 targeting clinical trials[17,18].

LIMITATIONS

Although the physiological concentrations of Aη peptides within the brain remain unknown, several lines of evidence suggest that our findings may reflect the physiological endogenous activity of these peptides *in vivo*. Previous data has indicated that the range of Aβ concentrations in rodents and humans to be within the high picomolar range, with CSF levels of $Aβ_{1-40}$ in healthy humans estimated to be around 1.5 nM[12,19–21]. We have also previously estimated endogenous Aη−α levels to be five-fold higher in CSF than Aβ[3], suggesting that Aη CSF levels might be expressed in the region of 7.5 nM. The range of 1–10 nM, for which we observed an impact of Aη on synapses, seems therefore within the estimated realm of the endogenous concentration of this peptide. It is thus conceivable that our observations reflect a novel form of physiological regulation of post-synaptic plasticity mechanisms by these peptides as a consequence of expression levels fluctuations due to neuron activity.

Intriguingly, our finding that the recombinant form of Aη−β lowers LTP is at variance with that found in our previous study[3], despite the derivation procedure of recombinant Aη−β being similar as described here. Since we did not quantify the precise concentration of recombinant peptide in our earlier study, it is possible that concentration applied previously failed to reach the limit of detection for an effect on LTP. Alternatively, it is possible that other factors, such as high glycosylation, purity or degradation of samples may have confounded our previous results, which were mitigated in the current study through systematic quality control steps until application.

Conclusions

In conclusion, we demonstrate that both Aη peptides acutely regulate neuronal mechanisms *ex vivo* and *in vivo* and could thus represent important endogenous modulators of synapse communication. Our findings provide further evidence that, beyond Aβ, APP cleavage products contribute to a rich array of effects on neuronal function[22], which delicately maintains neuronal network homeostasis and may be uniquely susceptible to perturbation.

List Of Abbreviations

aCSF artificial cerebrospinal fluid

AD Alzheimer's disease

APP Amyloid precursor protein

BACE1 β-secretase-1 cleavage site

CSF cerebrospinal fluid

DMSO dimethyl sulfoxide

ECL enhanced chemiluminescence

fEPSPs Field excitatory post-synaptic potentials

HEPES 4-(2-hydroxyethyl)-1-piperazineethanesulfonic acid

HFS high frequency stimulation

ISI inter stimulus interval

LTP long-term potentiation

MT1/5-MMP membrane types 1 and 5 matrix metalloproteinases

PBS phosphate buffered saline

Rec recombinant

ROIs Regions of interest

s synthetic

SD standard deviation

SEM standard deviation of the mean

TBS theta-burst stimulation

Declarations

Ethics approval and consent to participate

For *ex vivo* electrophysiology recordings, experiments were conducted according to the policies on the care and use of laboratory animals stipulated by French ministry of research according to the European Communities Council Directive (2010/63).

For *in vivo* LTP experiments, experiments were performed in accordance with local institutional and governmental regulations regarding the use of laboratory animals at the University of Frankfurt as approved by the Regierungspräsidium Darmstadt and the animal welfare officer responsible for the institution.

For *in vivo* calcium imaging experiments, experiments were conducted in compliance with institutional (Technische Universität München) animal welfare guidelines and approved by the state government of Bavaria, Germany.

Consent for publication

Not applicable.

Availability of data and materials

The datasets used and/or analyzed during the current study are available from the corresponding author on reasonable request.

Competing interests

The authors declare that they have no competing interests.

Funding

This work was funded by the French Government (National Research Agency, ANR) through the “Investments for the Future” LABEX SIGNALIFE : program reference # ANR-11-LABX-0028-01 to HM and MM, the Fondation Alzheimer to HM, the Association France Alzheimer (AAP SM 2018 #1795) to HM and the University of Toronto’s PEY, an internship program for undergraduates to YSM. This work was also supported by the Deutsche Forschungsgemeinschaft (German Research Foundation) within the framework of the Munich Cluster for Systems Neurology (EXC 2145 SyNergy) to YSM. This work was also supported by Alzheimer Forschung Initiative e.V. (15038) to PJ. SSH and MAB are supported by the UK Dementia Research Institute which receives its funding from DRI Ltd, funded by the Medical Research Council, Alzheimer's Society and Alzheimer Research UK. MAB is further supported by a UKRI Future Leaders Fellowship (Grant Number: MR/S017003/1) and acknowledges the donors of Alzheimer's Disease Research (ADR), a program of BrightFocus Foundation (Grant Number: A2019112S).

Authors' contributions

MM, JD, YSM, PP and HM performed and analyzed *ex vivo* electrophysiology experiments. JD performed protein analysis. MW together with CG designed the synthetic peptides, generated the recombinant peptides and provided intellectual inputs. MAB and SSH acquired and analyzed *in vivo* calcium imaging data. AB and AA performed and analyzed *in vivo* electrophysiology experiments supervised by PJ. HM wrote manuscript with help of other authors.

Acknowledgements

We are grateful for excellent technical assistance by Heike Hampel, Veronika Müller and Brigitte Nuscher (LMU Munich).

Authors' information

None.

References

1. van der Kant, R. & Goldstein, L. S. B. Cellular functions of the amyloid precursor protein from development to dementia. *Dev. Cell***32**, 502–515 (2015). doi: 10.1016/j.devcel.2015.01.022
2. Haass, C., Kaether, C., Thinakaran, G. & Sisodia, S. Trafficking and proteolytic processing of APP. *Cold Spring Harb Perspect Med***2**, a006270 (2012). doi: 10.1101/cshperspect.a006270
3. Willem, M. *et al.* eta-Secretase processing of APP inhibits neuronal activity in the hippocampus. *Nature***526**, 443–447 (2015). doi:10.1038/nature14864
4. Selkoe, D. J. Alzheimer's disease is a synaptic failure. *Science***298**, 789–791 (2002). doi: 10.1126/science.1074069
5. De Strooper, B. & Karran, E. The Cellular Phase of Alzheimer's Disease. *Cell***164**, 603–615 (2016). doi: 10.1016/j.cell.2015.12.056
6. Frere, S. & Slutsky, I. Alzheimer's Disease: From Firing Instability to Homeostasis Network Collapse. *Neuron***97**, 32–58 (2018). doi: 10.1016/j.neuron.2017.11.028
7. Taylor, C. J. *et al.* Endogenous secreted amyloid precursor protein-alpha regulates hippocampal NMDA receptor function, long-term potentiation and spatial memory. *Neurobiol. Dis.***31**, 250–260 (2008). doi: 10.1016/j.nbd.2008.04.011
8. Busche, M. A. *et al.* Critical role of soluble amyloid-beta for early hippocampal hyperactivity in a mouse model of Alzheimer's disease. *Proc.Natl.Acad.Sci.U.S.A***109**, 8740–8745 (2012). doi: 10.1073/pnas.1206171109
9. Stosiek, C., Garaschuk, O., Holthoff, K. & Konnerth, A. In vivo two-photon calcium imaging of neuronal networks. *Proc. Natl. Acad. Sci. U.S.A.***100**, 7319–7324 (2003). doi: 10.1073/pnas.1232232100
10. Jedlicka, P. *et al.* Neuroligin-1 regulates excitatory synaptic transmission, LTP and EPSP-spike coupling in the dentate gyrus in vivo. *Brain Struct Funct***220**, 47–58 (2015). doi: 10.1007/s00429-013-0636-1
11. Vnencak, M. *et al.* Lack of β-amyloid cleaving enzyme-1 (BACE1) impairs long-term synaptic plasticity but enhances granule cell excitability and oscillatory activity in the dentate gyrus in vivo. *Brain Struct Funct***224**, 1279–1290 (2019). doi: 10.1007/s00429-019-01836-6
12. Puzzo, D. *et al.* Picomolar amyloid-beta positively modulates synaptic plasticity and memory in hippocampus. *J.Neurosci.***28**, 14537–14545 (2008). doi: 10.1523/JNEUROSCI.2692-08.2008
13. Townsend, M., Shankar, G. M., Mehta, T., Walsh, D. M. & Selkoe, D. J. Effects of secreted oligomers of amyloid beta-protein on hippocampal synaptic plasticity: a potent role for trimers. *J.Physiol***572**, 477–492 (2006). doi: 10.3233/JAD-2012-129033. doi: 10.1113/jphysiol.2005.103754
14. Shankar, G. M. *et al.* Amyloid-beta protein dimers isolated directly from Alzheimer's brains impair synaptic plasticity and memory. *Nat.Med.***14**, 837–842 (2008). doi: 10.1038/nm1782
15. Li, S. *et al.* Soluble oligomers of amyloid Beta protein facilitate hippocampal long-term depression by disrupting neuronal glutamate uptake. *Neuron***62**, 788–801 (2009). doi: 10.1016/j.neuron.2009.05.012
16. Rice, H. C. *et al.* Secreted amyloid-β precursor protein functions as a GABABR1a ligand to modulate synaptic transmission. *Science***363**, (2019). doi: 10.1126/science.aao4827
17. Egan, M. F. *et al.* Randomized Trial of Verubecestat for Mild-to-Moderate Alzheimer's Disease. *N. Engl. J. Med.***378**, 1691–1703 (2018). doi: 10.1056/NEJMoa1706441
18. Egan, M. F. *et al.* Randomized Trial of Verubecestat for Prodromal Alzheimer's Disease. *N. Engl. J. Med.***380**, 1408–1420 (2019). doi: 10.1056/NEJMoa1812840
19. Schmidt, S. D., Nixon, R. A. & Mathews, P. M. ELISA method for measurement of amyloid-beta levels. *Methods Mol. Biol.***299**, 279–297 (2005). doi: 10.1385/1-59259-874-9:279
20. Giedraitis, V. *et al.* The normal equilibrium between CSF and plasma amyloid beta levels is disrupted in Alzheimer's disease. *Neurosci. Lett.***427**, 127–131 (2007). doi: 10.1016/j.neulet.2007.09.023
21. Puzzo, D. & Arancio, O. Amyloid-β Peptide: Dr. Jekyll or Mr. Hyde? *J Alzheimers Dis***33**, S111–S120 (2013). doi: 10.3233/JAD-2012-129033

22. Harris, S. S., Wolf, F., De Strooper, B. & Busche, M. A. Tipping the Scales: Peptide-Dependent Dysregulation of Neural Circuit Dynamics in Alzheimer's Disease. *Neuron***107**, 417–435 (2020). doi: 10.1016/j.neuron.2020.06.005

Figures

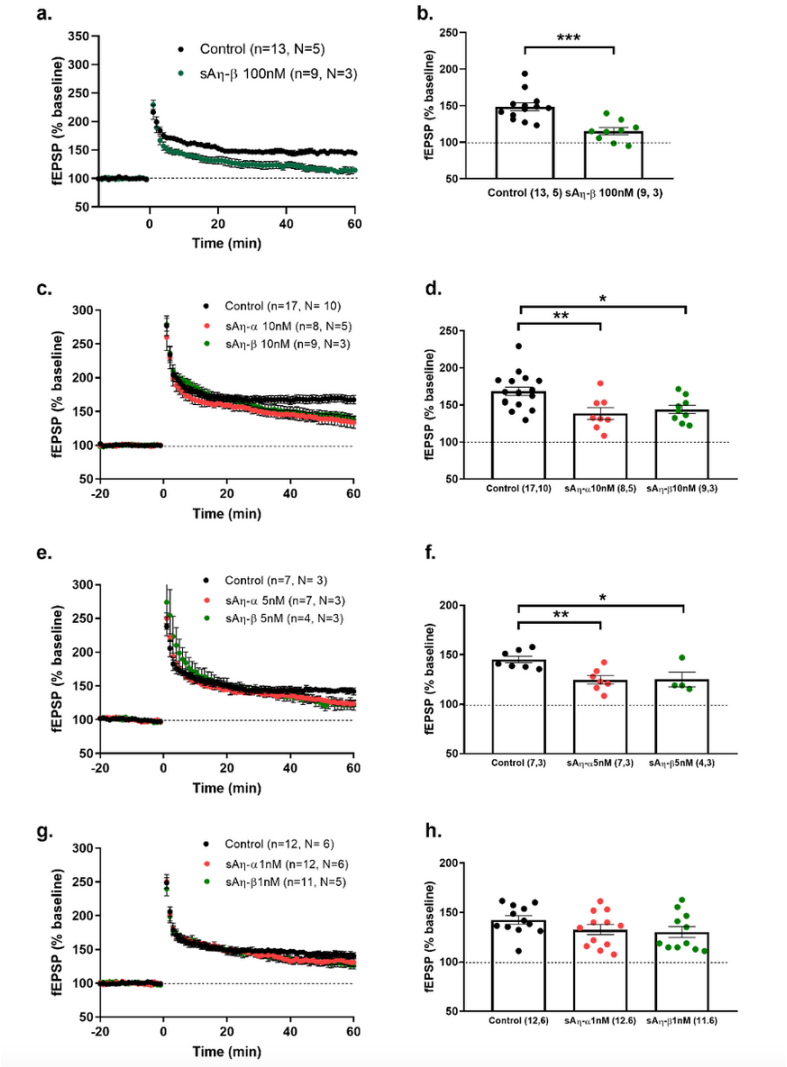

Figure 1

Synthetic Aη-α and Aη-β acutely inhibit LTP within the low nanomolar range a) Summary graphs of fEPSP slope (% baseline) pre- and post-LTP induction (time 0) in control or upon 15 min incubation with 100 nM sAη−β. b) Summary of fEPSP magnitude 45–60 min after LTP induction as fEPSP (% baseline) for data shown in a. c) Summary graphs of fEPSP slope (% baseline) pre- and post-LTP induction (time 0) in control or upon 20 min incubation with 10 nM sAη−α or sAη−β. d) Summary of fEPSP magnitude 45–60 min after LTP induction as fEPSP (% baseline) for data shown in c. e) Summary graphs of fEPSP slope (% baseline) pre- and post-LTP induction (time 0) in control or upon 20 min incubation with 5 nM sAη−α or sAη−β. f) Summary of fEPSP magnitude 45–60 min after LTP induction as fEPSP (% baseline) for data shown in e. g) Summary graphs of fEPSP slope (% baseline) pre- and post-LTP induction (time 0) in control or upon 20 min incubation with 1 nM sAη−α or sAη−β. h) Summary of fEPSP magnitude 45–60 min after LTP induction as fEPSP (% baseline) for data shown in g. (n= slices, N= mice), *p<0.05,**p<0.01, ***p<0.001. Detailed statistics are shown in Supplementary Table S1.

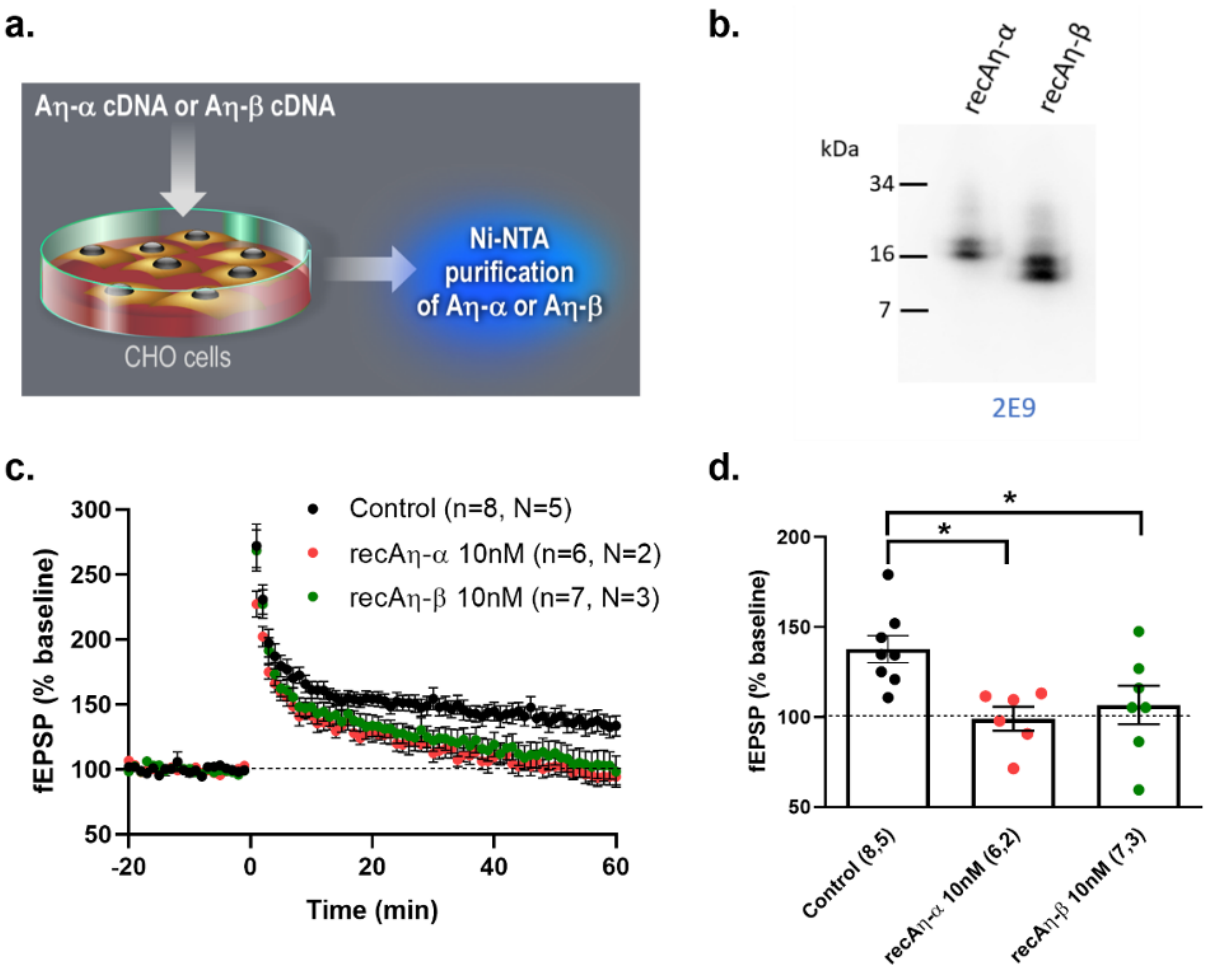

Figure 2

10 nM of soluble recombinant Aη−α and Aη−β lower LTP a) Diagram explaining production of soluble HIS-tagged recAη−α and recAη−β samples used in b-d (see methods for details of Ni-NTA purification and sample quantification). b) 10ng of purified recAη−α and recAη−β peptides were blotted with 2E9 antibody. c) Summary graphs of fEPSP slope (% baseline) pre- and post-LTP induction (time 0) in control or upon 20 min incubation with 10 nM recAη−α or recAη−β. d) Summary of fEPSP magnitude 45–60 min after LTP induction as fEPSP (% baseline) for data shown in c. (n= slices, N= mice), *p<0.05. Detailed statistics are shown in Supplementary Table S2.

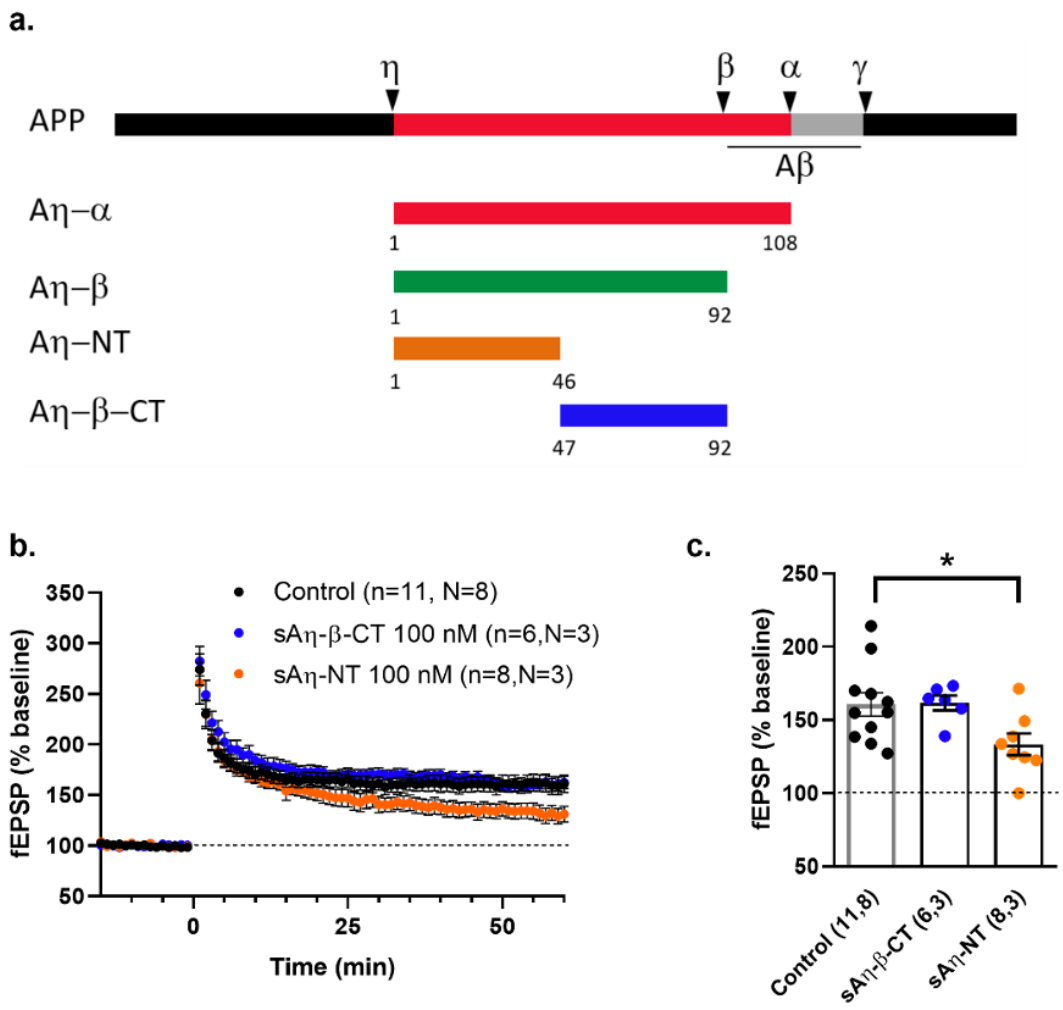

Figure 3

N-terminal of Aη is necessary and sufficient for LTP impairment. a) Diagram showing APP processing (secretases cleavage sites are shown) and boundaries of shorter synthetic peptides used to identify active site. b) Summary graphs of fEPSP slope (% baseline) pre- and post-LTP induction (time 0) in control or upon 20 min incubation with 100 nM sAη–NT or sAη–β-CT. c) Summary of fEPSP magnitude 45–60 min after LTP induction as fEPSP (% baseline) for data shown in b. (n= slices, N= mice), *p<0.05. Detailed statistics are shown in Supplementary Table S3.

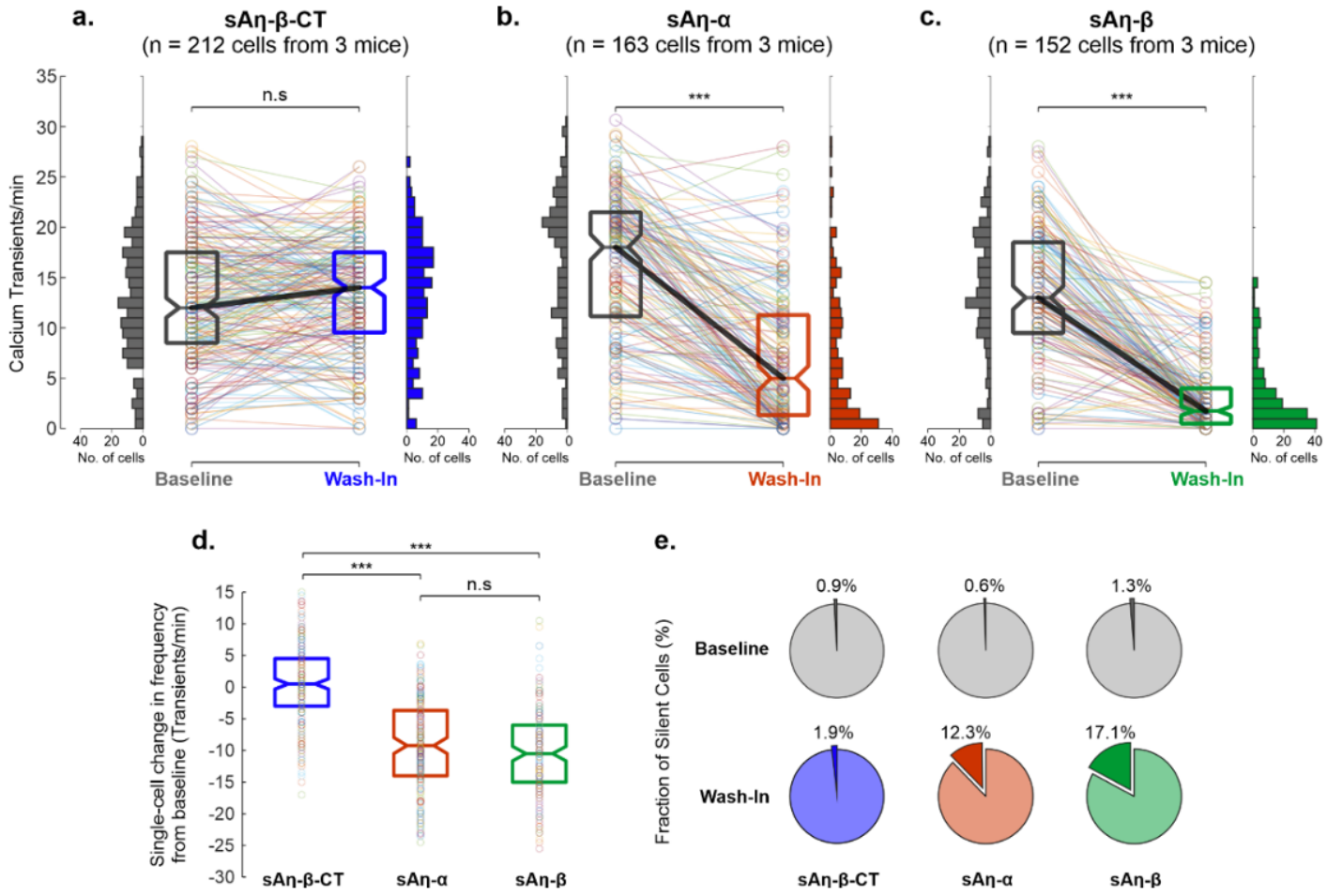

Figure 4

Synthetic Aη-α and Aη-β acutely modulate neuronal activity in vivo. a) The median frequency of calcium transients did not differ significantly (n.s) from baseline following superfusion (wash-in, blue) of sAη−β−CT (control peptide). Note the high degree of similarity in distribution of calcium transient frequencies as denoted by the upright histograms. The frequency of calcium transients for each individual neuron before (baseline) and after superfusion (wash-in) of sAη−β−CT is overlaid. b) Superfusion of sAη−α (wash-in, red) induced a significant decrease in median calcium transient frequency and a positive skew in the distribution of calcium transient frequencies towards hypoexcitability. The frequency of calcium transients for each individual neuron before (baseline) and after superfusion (wash-in) of sAη−α is overlaid. c) Superfusion of sAη−β (wash-in, green) also induced a significant decrease in median calcium transient frequency and a positive skew in the distribution of calcium transient frequencies towards hypoexcitability. The frequency of calcium transients for each individual neuron before (baseline) and after superfusion (wash-in) of sAη−β is overlaid. d) Across all individual cells studied, the median change in calcium transient frequency following superfusion of sAη−α (red) and sAη−β (green) was not statistically different (n.s), but were significantly lower relative to the null change associated with sAη−β−CT (blue). The change in calcium transient frequency for each individual neuron after superfusion (wash-in) of each peptide is overlaid. e) While the proportion of silent neurons (i.e. showing absence of calcium transients) were small during baseline conditions (grey charts), and following sAη−β−CT superfusion (wash-in, blue), superfusion of sAη−α (wash-in, red) and sAη−β (wash-in, green) was associated with a dramatic increase in the number of inactive cells. For each boxplot, the central line denotes the median with bottom and top demarcations indicating the 25th and 75th percentiles, respectively. ***p<0.001. Detailed statistics are shown in Supplementary Table S4.

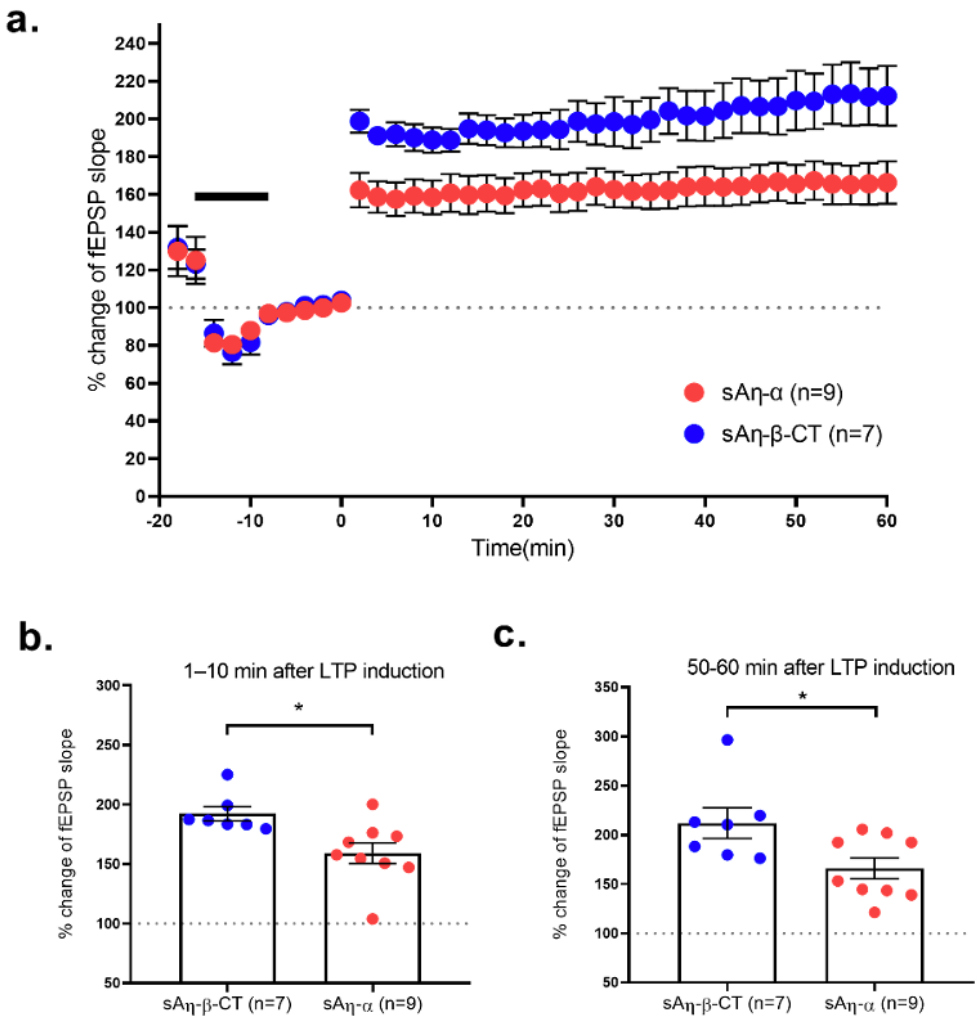

Figure 5

sAη−α acutely lowers LTP in vivo. a) Summary graphs of fEPSP slope (% baseline) pre- and post-LTP induction (time 0) upon 10 min of intra-hippocampal injection of 1 μM of a control peptide (sAη−β−CT) or a sAη−α peptide. Injection time is shown by the black bar. Note a transient decline and partial recovery of baseline responses upon the injection and a subsequent LTP induction. b) Summary of fEPSP magnitude 1–10 min after LTP induction as fEPSP (% baseline) for data shown in a. c) Summary of fEPSP magnitude 50–60 min after LTP induction as fEPSP (% baseline) for data shown in a. All recordings were done in vivo in Sprague Dawley rats with n= number of rats. *p<0.05 Detailed statistics are shown in Supplementary Table S5.

Supplementary Files

This is a list of supplementary files associated with this preprint. Click to download.

- Menschetalsupplementarymaterial.pdf